Discovery of Novel Antitumor Antimitotic Agents That Also Reverse Tumor Resistance[1]

Aleem Gangjee,*,† Jianming Yu,† Jean E. Copper,‡ and Charles D. Smith‡

Division of Medicinal Chemistry, Graduate School of Pharmaceutical Sciences, Duquesne University, Pittsburgh, Pennsylvania 15282, and Department of Pharmaceutical Sciences, College of Pharmacy, Medical University of South Carolina, Charleston, South Carolina 29425

Received February 20, 2007

We have discovered a novel series of 7-benzyl-4-methyl-5-[(2-substituted phenyl)ethyl]-7*H*-pyrrolo[2,3-*d*]-pyrimidin-2-amines, which possess antimitotic and antitumor activities against antimitotic-sensitive as well as resistant tumor cells. These agents bind to a site on tubulin that is distinct from the colchicine, vinca alkaloid, and paclitaxel binding sites and some, in addition to their antitumor activity, remarkably also reverse tumor resistance to antimitotic agents mediated via the P-glycoprotein efflux pump. The compounds were synthesized from *N*-(7-benzyl-5-ethynyl-4-methyl-7*H*-pyrrolo[2,3-*d*]pyrimidin-2-yl)-2,2-dimethylpropanamide **11** or the corresponding 5-iodo analog **14** via Sonogashira couplings with appropriate iodobenzenes or phenylacetylene followed by reduction and deprotection to afford the target analogs. Sodium and liquid NH_3 afforded the debenzylated analogs. The most potent analog **1** was one to three digit nanomolar against the growth of both sensitive and resistant tumor cells in culture. Compounds of this series are promising novel antimitotic agents that have the potential for treating both sensitive and resistant tumors.

Introduction

Microtubules are long, protein polymers that are formed by α-tubulin and *β*-tubulin heterodimers. These heterodimers first form a short microtubule nucleus followed by elongation and arrangement in the form of tubes. The polymerization of microtubules occurs via complex polymerization dynamics that involves GTP hydrolysis to supply energy at the time that tubulin, with bound GTP, adds to the microtubule ends. In mitosis, the duplicated chromosomes of cells are divided into two identical sets prior to division into two daughter cells, and the polymerization dynamics of microtubules plays a pivotal role in this process as part of cell replication.[2,3] The crucial involvement of microtubules in mitosis makes them a target for antitumor agents.

In general, antitumor agents that inhibit the function of microtubules are known as antimitotic agents. Classification of antimitotic agents is by their mechanisms of action and their different binding sites on tubulin. Three distinct classes of antimitotic agents are identified. The *Vinca* alkaloids exemplified by vincristine, vinblastine, vindesine, and vinorelbine (Chart 1). These are *β*-tubulin binding agents that interfere with proper mitotic spindle formation by preventing the normal dynamics and polymerization of spindle microtubule formation. The *Vinca* alkaloids are important in the treatment of leukemias, lymphomas, small cell lung cancer, and other cancers.[3,4] These agents are also known as microtubule-destabilizing agents or microtubule polymerization inhibitors or depolymerizers. The second group are the taxanes exemplified by paclitaxel (Chart 1) and docetaxel (Chart 1). The binding site for paclitaxel is in the *β*-subunit as well, however, its location is different from that of the *Vinca* alkaloids. Paclitaxel binds on the inside surface of the *β*-subunit in microtubule, as determined in tubulin protofilaments in Zn sheets.[5,6] Paclitaxel increases microtubule polymerization and thus interferes with spindle microtubule dynamics and prevents the dividing cell from progression. These are microtubule-stabilizing agents or polymerizing agents. The taxanes are clinically useful in the treatment of breast, lung, ovarian, head and neck, and bladder carcinomas among others. The third class typified by colchicine (Chart 1) is comprised of a diverse collection of small molecules that bind to the colchicine binding site. The nature of this binding site has not been determined with certainty, however, insights into the colchicine binding sites are available from homology models.[7] These compounds are microtubule polymerization inhibitors similar to the *Vinca* alkaloids, but their binding is on a different site and their depolymerization mechanism of action is also different. Combretastatins (Chart 1) are a class of drugs that are in clinical trials as antitumor agents that bind to the colchicine binding site.[2] Colchicine itself is not used as an antitumor agent, but is used in gout. It has also recently been recognized that some antimitotic agents rapidly shut down existing tumor vasculature.[7,8] This is shown for the taxanes, colchicine, *Vinca* alkaloids, as well as combretastatins. This effect is different from the antiangiogenesis effect of inhibition of receptor tyrosine kinases (RTKs[a]).

Multidrug or multiple drug resistance (MDR) is a major drawback of cancer chemotherapy, including the clinically used antimitotic agents. These arise from intrinsic or acquired mechanisms of resistance. A major mechanism of MDR occurs via an overexpression of energy dependent (ATP), unidirectional transmembrane efflux pumps. Ultimate failure of chemotherapy with antimitotic drugs often results due to MDR. P-glycoprotein (Pgp) is a 170 kDa protein that belongs to the ATP-binding cassette superfamily of transporters.[9−11] A series of homologous proteins termed multidrug-resistance proteins (MRPs) have also been reported.[12,13] The first MRP termed MRP1 was identified in a drug resistant lung cancer cell line that does not express Pgp.[14] All these transporters bind drugs within the cell and release them to the extracellular space using ATP.[14,15] Tumor cells pre-exposed to cytotoxic compounds often overexpress

* To whom correspondence should be addressed. Telephone: 412-396-6070. Fax: 412-396-5593. E-mail: gangjee@duq.edu.
† Duquesne University.
‡ Medical University of South Carolina.

[a] Abbreviations: MDR, multiple drug resistance; Pgp, P-glycoprotein; MRP, multidrug-resistance proteins; PCC, Pearson correlation coefficients; SRB, sulforhodamine B; RTK, receptor tyrosine kinase; MTP, microtubule protein; TLC, thin layer chromatography; NMR, nuclear magnetic resonance; EGFR, endothelial growth factor receptor; VEGFR, vascular endothelial growth factor receptor; PDGFR, platelet-derived growth factor receptor; IGF1-R, insulin growth factor 1-receptor; NCI, National Cancer Institute.

10.1021/jm070194u CCC: $37.00
Published on Web 06/14/2007

Chart 1

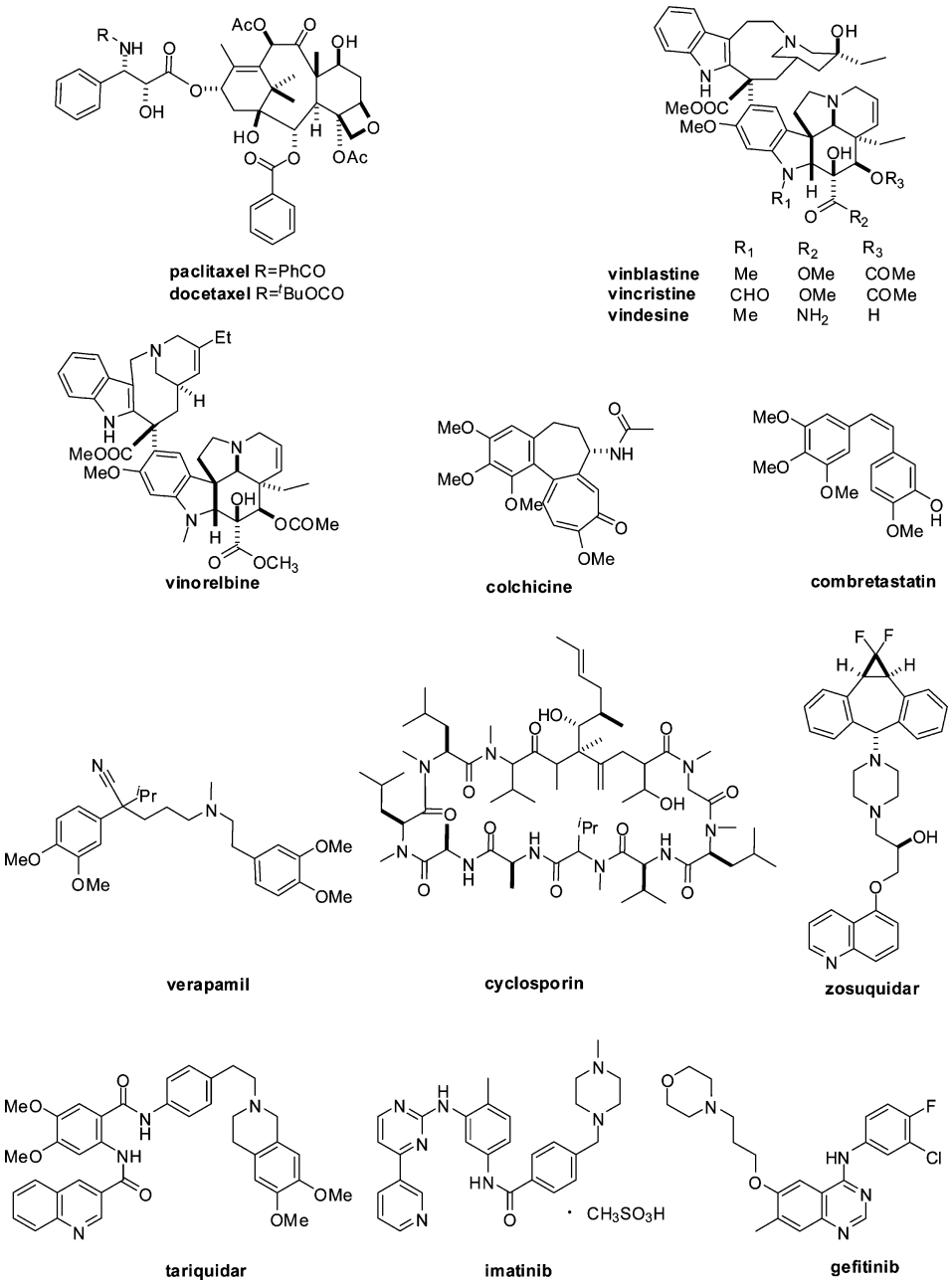

these pumps, which allows the cells to manifest resistance in the presence of the cytotoxic drug. MDR affects cancer patients with leukemias as well as solid tumors. Overexpression of Pgp has been reported in a number of tumor types, particularly after the patient has received chemotherapy, indicating the clinical importance of Pgp in MDR.[10,16−19] In addition, it has also been reported that Pgp expression may be a prognostic indicator in certain cancers and is associated with poor response to chemotherapy.[20,21] MRP1 overexpression is not consistently found in tumors even though it is expressed in a high percentage of leukemias and solid tumors.[22] It has also been shown that the MRP1 mRNA levels in malignant melanoma,[23] acute lymphocytic leukemia,[24] or chronic lymphocytic leukemia[31] were not altered by chemotherapy. Thus overexpression of Pgp appears to be more relevant in the clinical setting than elevation of MRP1 levels.

The clinical significance of Pgp along with its limited expression in normal tissues makes Pgp a viable target for inhibition to reverse MDR. Several Pgp inhibitors or modulators have been developed to reverse MDR that occur for chemotherapeutic agents in general and include antimitotic inhibitors. Notable among these are verapamil[25] and cyclosporine[11,25] (Chart 1) and, more recently, tariquidar[26,27] (Chart 1) and zosuquidar[28] (Chart 1), which have improved selectivity. The variety of structural types of agents that have MDR inhibitory effects can be found in the comprehensive review by Avendaño and Menéndez.[29] Though the three-dimensional (3-D) structure of Pgp is not available at high resolution, several attempts have been made at determining structure function relationships of MDR Pgp and predicting Pgp substrate structure−activity relationships, the most recent of these is described by Pajeva et al.[30] and Gombar et al.,[31] respectively. In addition, structural models have also been proposed based on the *E. coli* MsbA lipid transporter.[32] Recently, a low-resolution 3-D structure of mammalian Pgp at 20 Å has been reported[33] and indicates ATP binding causes a conformational change in the structure, resulting in repacking into three compact domains.

Scheme 1[a]

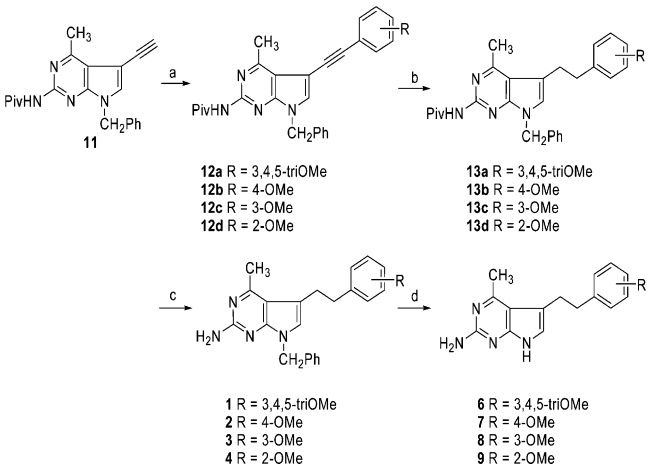

[a] Reagents and conditions: (a) substituted iodobenzene, tetrakis(triphenylphosphine)palladium(0), triethylamine, CuI, rt, dark, dichloroethane; (b) 5% Pd/C, 50 psi, H_2; (c) 1 N NaOH, MeOH, 80 °C; (d) Na/liq NH_3, −78 °C.

Scheme 2[a]

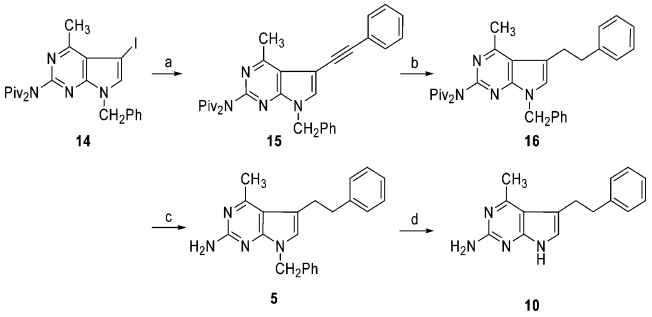

[a] Reagents and conditions: (a) phenylacetylene, triethylamine, tetrakis(triphenylphosphine)palladium(0), CuI, rt, dark, dichloroethane; (b) 5% Pd/C, 50 psi, H_2; (c) 1 N NaOH, MeOH, 80 °C; (d) Na/liq NH_3, −78 °C.

Though antimitotic agents have shown to be some of the most successful agents against malignancies, resistance, both intrinsic and acquired, is of major concern and results in treatment failures. Thus, new agents that possess antimitotic and antitumor activities without substrate activity for Pgp are highly coveted and would be useful antitumor agents as single agents or in combination with chemotherapeutic agents, including antimitotic agents.

We have been extensively involved in the synthesis of fused heterocyclic analogs and the structure-based design of inhibitors of RTK[34,35] and folate metabolizing enzymes.[36−38] These studies have afforded the synthesis of substituted furo[2,3-*d*]pyrimidines, pyrrolo[2,3-*d*]pyrimidines, and thieno[2,3-*d*]pyrimidines, among several other monocyclic, bicyclic, tricyclic, and tetracyclic heterocycles. Our interest in RTK inhibitors and the vast literature on the design and synthesis of such inhibitors, including the clinically used agents imatinib[39] (Chart 1) and gefitinib[39] (Chart 1), indicated that though the kinase binding sites all accommodate ATP, there are subtle differences in the ATP binding sites of the kinases such that, with rational design, inhibitors of kinases can be obtained with selectivity and specificity for a particular class and even a specific kinase.[34,35,39] We[40] had previously synthesized intermediate *N*-(7-benzyl-5-ethynyl-4-methyl-7*H*-pyrrolo[2,3-*d*]pyrimidin-2-yl)-2,2-dimethylpropanamide (**11**) and the corresponding 5-iodo analog (**14**; Schemes 1 and 2). Elaborations of **11** and **14** to potential RTK inhibitors with C5 and N7 substitutions could provide RTK inhibitors.

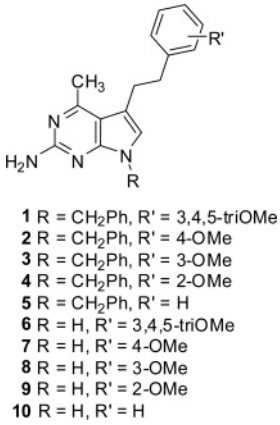

Thus, we synthesized compounds **1**−**5** (Scheme 1) and **6**−**10** initially as potential RTK inhibitors.

Chemistry

The synthesis of the target compounds **1**−**10** were accomplished as indicated in Schemes 1 and 2. For the synthesis of **6**−**9** (Scheme 1), we found that the N7-benzyl group was necessary to increase the solubility of the intermediates and, more importantly, facilitated the Sonogashira coupling reaction with acetylenes. Thus, we started with the *N*-benzylated analog **11**[40] (Scheme 1). Compound **11** was coupled using the Sonogashira reaction with appropriately substituted iodobenzenes in the presence of tetrakis(triphenylphosphine)palladium(0) ($Pd(PPh_3)_4$), copper(I) iodide (CuI), and triethylamine in dichloroethane. The reaction went to completion in 24 h, and the products **12a**−**d** were isolated in 48−79% yield. Subsequent catalytic hydrogenation of **12a**−**d**, with 3−4 drops of ammonium hydroxide (to prevent pyrrole reduction) and 5% palladium-on-charcoal in a mixture of methanol and dichloromethane (1:1), afforded **13a**−**d** in 67−91% yield. Hydrolysis with 1 N NaOH at 80 °C for 24 h afforded **1**−**4** in 79−90% yield. Debenzylation with sodium in liquid ammonia at −78 °C was found to be optimum and afforded compounds **6**−**9** in 19−48% yield (Scheme 1).

For the synthesis of the unsubstituted phenyl analogs **5** and **10**, compound **14**[40] was directly coupled with commercially available phenylacetylene using $Pd(PPh_3)_4$, CuI, and triethylamine to afford **15** in 78% yield (Scheme 2). The reaction sequences described in Scheme 1 were adopted for **15** to **16** and for the target compounds **5** and **10** (Scheme 2).

Biological Evaluation and Discussion

We discovered that some of the compounds **1**−**5**, which we had originally synthesized as potential RTK inhibitors, had antitumor activity against a variety of tumor cells but were not inhibitors of the RTKs evaluated (EGFR, VEGFR1 and 2, PDGFR-β, and IGF1-R). In the NCI[41] 60 cell line panel compound **1**, the 3,4,5-triOMe analog inhibited most of the cell lines with GI_{50} values that ranged from single digit nanomolar to submicromolar (Table 1). Compound **1** had a GI_{50} of single or two digit nanomolar activity against 16 tumor cell lines, GI_{50} of submicromolar levels against 40 of the other tumor cells, and micromolar levels against three tumor cells. Removal of the N7-benzyl group of **1** to afford **6** decreased activity by 100 to 10 000-fold against 56 tumor cell lines evaluated (data not shown), indicating the importance of the N7-benzyl moiety. The 3-OMe analog **3** showed GI_{50} values in the micromolar range for 8 of the 56 tumor cell lines and two digit nanomolar against a renal cancer A498 cell. The 2-OMe compound, **4**, was similar

Table 1. Tumor Cell Inhibitory Activity GI_{50} (nM) of Compound **1** (NCI)

panel/cell line	GI_{50}	panel/cell line	GI_{50}	panel/cell line	GI_{50}	panel/cell line	GI_{50}
leukemia		**colon cancer (ctd.)**		**melanoma (ctd.)**		**renal cancer (ctd.)**	
CCRF-CEM	58.0	HCC-2998	317	SK-MEL-2	381	RXF 393	134
HL-60(TB)	64.7	HCT-116	286	SK-MEL-28	>1000	SN12C	537
K-562	84.6	HCT-15	127	SK-MEL-5	61.1	TK10	961
MOLT-4	285	HT29	281	UACC-257	80.2	UO-31	347
RPMI-8226	439	KM12	194	UACC-62	39.9	**prostate cancer**	
SR	31.4	SW-620	236	**ovarian cancer**		PC-3	47.9
NSCLC		**CNS cancer**		IGROVI	61.1	DU-145	224
A549/ATCC	173	SF-268	669	OVCAR-3	28.8	**breast cancer**	
EKVX	424	SF-295	41.8	OVCAR-4	821	MCF7	118
HOP-92	467	SF-539	74.5	OVCAR-5	>1000	NCI/ADR-RES	145
NCI-H226	195	SNB-19	273	OVCAR-8	364	MDA-MB-231/ATCC	595
NCI-H23	278	SNB-75	358	SK−OV-3	506	HS 578T	283
NCI-H322M	581	U251	144	**renal cancer**		MDA-MB-435	10.1
NCI-H460	162	**melanoma**		786−0	254	MDA-N	<10.0
NCI-H522	47.7	LOX IMVI	250	A498	136	BT-549	>1000
colon cancer		MALME-3M	283	ACHN	728	T-47D	563
COLO 205	190	M14	77.0	CAKI-1	366		

Table 2. Compare Analysis Data for Compound **1**[a]

drug	correlation coefficient
vinblastine sulfate	0.748
paclitaxel	0.680
rhizoxin	0.677
maystansine	0.663
vincristine sulfate	0.635

[a] PCC values calculated by TGI_{50}.

Table 3. Cytotoxicity of Compounds **1**−**5**[a]

cmpd	T24	MCF-7 IC_{50} (μM)	NCI/ADR	MCF-7/VP
1	0.28 ± 0.10	0.30 ± 0.16	0.25 ± 0.12	0.25 ± 0.16
2	31.7 ± 1.7	13.0 ± 3.5	21.7 ± 4.4	22.7 ± 3.7
3	25.0 ± 2.9	8.0 ± 3.5	5.7 ± 0.7	22.0 ± 4.2
4	2.5 ± 0.3	2.3 ± 0.6	2.7 ± 0.4	2.6 ± 0.1
5	12.7 ± 2.3	10.7 ± 4.7	18.2 ± 7.4	18.3 ± 6.0

[a] The IC_{50} for each compound was determined as described in the Experimental Section. Values are expressed as μM and represent the mean ± SEM for three experiments.

to **3**, with activities (GI_{50}s) in the micromolar to millimolar range against the tumor cells in culture. The 4-OMe compound **2** inhibited the tumor cells at GI_{50} concentrations that were similar to **6**, indicating the importance of the 3- and/or 5-OMe groups. The phenyl unsubstituted analog **5** has GI_{50} values in the millimolar or less range for 52 of the tumor cells, with micromolar GI_{50} values for three of the tumor cell lines. Removal of the N7-benzyl group from any of the compounds substantially decreased activity against the 60 cell line panel. The tumor cell inhibitory activity from this limited 10 analog series indicated that the 3,4,5-triOMe substitution along with the presence of the N7-benzyl moiety afforded the most potent inhibitory activity against tumor cells in culture.

The NCI COMPARE analysis[42] was also performed for **1** to elucidate a possible mechanism of action of **1** by the similarity responses of the 60 cell lines to known compounds. The five compounds whose cell type selectivity profile showed the highest Pearson correlation coefficients (PCC)[43] with compound **1** were all well-known microtubule-targeting agents (Table 2). For microtubule specific compounds, the cell type selectivity profile in TGI level is highly indicative of the compound's mechanism of action. For a compound to be categorized in this class requires that (1) the PCC values should be at least 0.6 and (2) the average GI_{50} should be 1 μM or less.[44] Compound **1** satisfied both requirements indicating an antitubulin mechanism of action for **1**.

Cytotoxicity toward Sensitive and Resistant Tumor Cell Lines. The series of analogs **1**−**5** was also evaluated for cytotoxicity toward human tumor cell lines that included cell lines resistant to anticancer drugs due to overexpression of the transport proteins Pgp or MRP1 (Table 3). The unsubstituted phenyl ethyl compound **5** demonstrated IC_{50}s ranging from 11 to 18 μM. NCI/ADR cells that overexpress Pgp and MCF-7/VP cells that overexpress MRP1 had IC_{50}s slightly higher than the drug-sensitive MCF-7 cells. A 4-OMe substitution of the 5-phenylethyl moiety (compound **2**) decreased the cytotoxic potency toward T24 human bladder carcinoma cells but had little effect on the potency toward the other cell lines. Conversely, 3-OMe substitution (compound **3**) enhanced the potency toward NCI/ADR cells, and a 2-OMe substitution (compound **4**) substantially increased the potency toward all of the tested cell lines and eliminated any resistance due to overexpression of either Pgp or MRP1. Submicromolar cytotoxic potency was observed for the 3,4,5-triOMe compound **1**, again regardless of the transporter status of the cells. The data from Table 3 indicates that the 3,4,5-triOMe substitution is important for potent activity. Among the mono-OMe analogs, the 2-OMe is better than the 3-OMe and the 4-OMe. However, the unsubstituted phenyl analog is better than a mono-3- or -4-OMe substitution. Thus, the triOMe analog **1** is 10-fold better than **4** (2-OMe), which in turn is about 10 times better than the 3- or 4-OMe and 5 times better than the unsubstituted phenyl analog **5**.

Because of the effects of the compounds on microtubules (discussed below), the cytotoxic activity of **1** was compared with the microtubule-targeting drugs paclitaxel, vinblastine, and vincristine (Table 4). Although each of these natural product drugs were more potent than **1** in the sensitive cell line, each was subject to tumor cell resistance due to the overexpression of Pgp. Additionally, overexpression of MRP1 (MCF-7/VP) also confers substantial resistance to vincristine. In contrast, the observation that neither Pgp nor MRP1 affect cell sensitivity to **1** was confirmed. Compound **1** was 35- to 40-fold more potent than the established anticancer drug cisplatin, which is also insensitive to transporter expression by the tumor cells.

Effects of 1 on Microtubule Structure. The morphological effects of **1** on cultured cells and the NCI COMPARE analysis results described above suggested that the effects of vinblastine, paclitaxel, and **1** on microtubule structure should be examined. For these studies, A-10 rat smooth muscle cells were used because they grow as flat monolayers that are amenable to imaging. None of these compounds affected the morphology

Table 4. Effects of Pgp and MRP1 on Drug Sensitivity[a]

drug	MCF-7 Pgp−/MRP1 IC_{50}	NCI/ADR Pgp+/MRP1 IC_{50}	resistance factor	MCF-7/VP Pgp−/MRP1+ IC_{50}	resistance factor
paclitaxel (nM)	2.5 ± 0.6	2700 ± 500	1080	2.8 ± 0.6	1.1
vinblastine (nM)	2.8 ± 0.5	>375	>134	3.0 ± 0.6	1.1
vincristine (nM)	0.6 ± 0.1	100	167	9.3 ± 1.4	15.5
cisplatin (μM)	11.5 ± 4.1	12.2 ± 4.2	1.1	7.0 ± 2.9	0.6
1 (μM)	0.28 ± 0.01	0.35 ± 0.04	1.3	0.18 ± 0.01	0.6

[a] The IC_{50} for each compound was determined as described in Experimental Section. Values expressed are the mean ± SEM for three experiments.

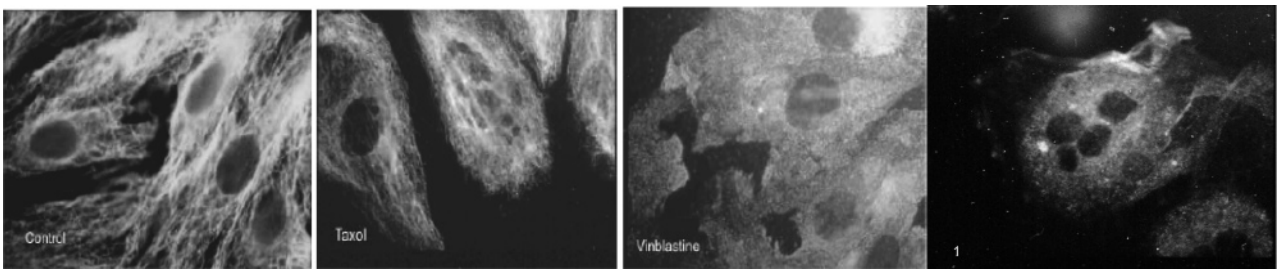

Figure 1. Microtubule structure in A-10 cells. A-10 cells were treated for 24 h with EtOH (control), 625 nM paclitaxel, 167 nM vinblastine, or 900 nM **1** (compound **1** in Figure 2). Microtubules were then visualized by indirect immunofluoesence staining with β-tubulin antibodies. Representative fields are shown.

Table 5. Effects of **1** and Antimicrotubule Drugs on the Cell Cycle Distribution of HL-60 Cells

treatment	G_0/G_1	S	G_2/M
control	78.5 ± 0.0	16.6 ± 0.2	4.9 ± 0.2
paclitaxel (200 nM)	67.3 ± 0.4	22.2 ± 0.4	10.5 ± 0.1
vinblastine (80 nM)	83.3 ± 1.3	6.6 ± 1.6	10.1 ± 0.3
colchicine (600 nM)	84.1 ± 0.7	4.0 ± 1.4	11.9 ± 0.3
1 (6 μM)	80.0 ± 2.4	10.3 ± 2.0	9.7 ± 0.4

of stress fibers composed of microfilaments (data not shown). Control cells displayed extensive microtubule systems with perinuclear organizing centers (Figure 1). Treatment with paclitaxel promoted increased staining of microtubule clusters in these cells, while vinblastine caused marked depletion of cellular microtubules. Similarly, **1** (Figure 1) caused dose-dependent losses of microtubules in the cells. Like paclitaxel, many cells with aberrant nuclei were observed in cultures treated with **1**. Similar losses of microtubules were observed in cultures of NIH/3T3 and MCF-7 cells treated with **1** (data not shown).

Cell Cycle Effects of 1. Flow cytometric analyses were used to assess the effects of **1** and antimicrotubule drugs on the cell cycle phase distributions of HL-60 human promyelocytic leukemia cells. The percentages of cells in the G_2/M phases were increased approximately 2-fold by treatment of the cells for 24 h with either paclitaxel, vinblastine, colchicine, or **1** (Table 5). Increasing the incubation time to 48 h did not substantially increase the percentage of cells arrested in G_2/M for any of the compounds; however, the percentage of subdiploid cells was increased in each sample, indicating the induction of apoptosis by these compounds (data not shown).

To further characterize the cell cycle effects of **1** on human tumor cells, MCF-7 cells were treated with **1**, vinblastine, or paclitaxel, and the expression of p53 and WAF1 were examined by immunoblotting. Arrest of these cells in G_2/M by antimicrotubule drugs has previously been demonstrated to correlate with increased expression of these proteins. As predicted, treatment with paclitaxel or vinblastine resulted in marked increases in the levels of expression of both p53 and WAF1 (Figure 2). Similarly, treatment with **1** induced the expression of both of these proteins. None of these treatments affected the expression of bcl-2 or β-tubulin in the MCF-7 cells (data not shown).

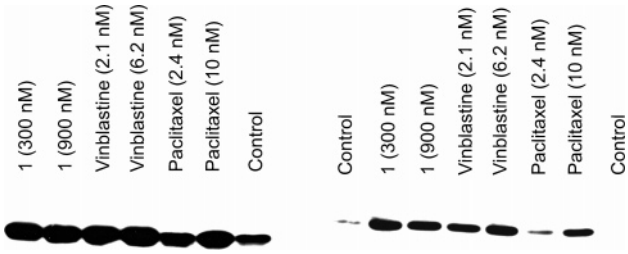

Figure 2. Expression of p53 and Waf-1 in MCF-7 cells. MCF-7 cells were treated for 24 h with the indicated concentrations of EtOH (control), paclitaxel, vinblastine, or **1** (compound 149 in Figure 3). Cells were then harvested, lysed, and analyzed for levels of expression of p53 (left) or Waf-1 (right) by Western Blot analyses. Data from one of two similar experiments is shown.

Effects of Compounds 1−5 on Pgp-Mediated Multiple Drug Resistance. Studies described above in Tables 3 and 4 indicated that expression of Pgp or MRP1 does not confer resistance to the cytotoxic effects of the compounds. To determine if this is due to inhibition of drug transport activity by these proteins, the effects of these compounds on Pgp were further characterized. The effects of the compounds on the sensitivity of NCI/ADR cells to vinblastine and of MCF-7/VP cells to vincristine were examined to evaluate antagonism of Pgp and MRP1, respectively. As indicated in Figure 3 (left panel), increasing doses of either **2**, **3**, **4**, or **5** caused dose-dependent sensitization of NCI/ADR cells to vinblastine, indicating inhibition of Pgp. Compound **4** was approximately 10-fold more potent than the others in reversing Pgp-mediated resistance. Apparent decreases in this activity by high doses of the compounds are due to direct cytotoxicity of the compound, thereby lowering the ratio of survival in the absence of vinblastine relative to survival in the presence of vinblastine. Compound **1** was significantly more cytotoxic than the others in the series, but had no affect on Pgp at doses below its IC_{50}. In contrast with the marked effects on Pgp-mediated resistance, none of the compounds affected the ability of vincristine to kill MCF-7/VP cells, indicating that they are ineffective in blocking the actions of MRP1. Overall, these data demonstrate that *ortho*-OMe substitution of the 5-phenyl ethyl moiety (compound **4**) of this series greatly enhances its ability to inhibit Pgp, whereas further substitution (3,4,5-triOMe in **1**) may negate this effect

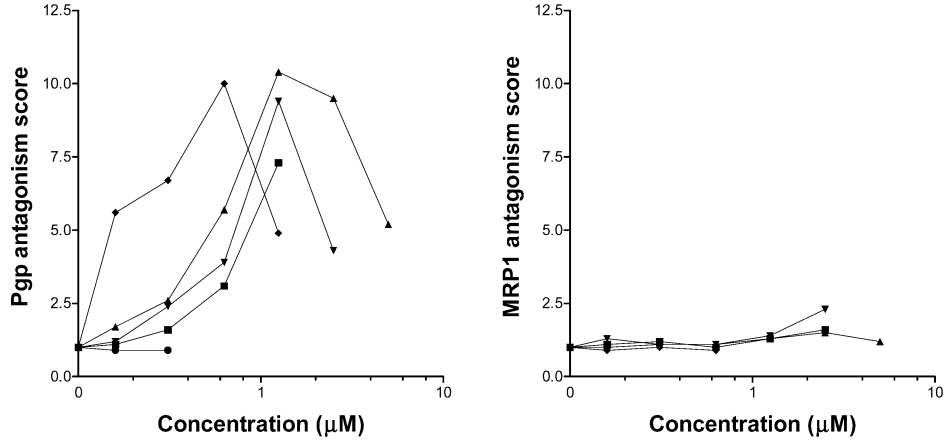

Figure 3. Compounds **1**−**5** reverse Pgp-mediated drug resistance but not MRP1-mediated drug resistance. Left panel: NCI/ADR cells were treated with the indicated concentrations of **5** (■), **2** (▲), **3** (▼), **4** (♦), or **1** (●) either in the absence or in the presence of 50 nM vinblastine. The Pgp antagonism score is calculated as the percentage survival of cells in the absence of vinblastine/percentage survival in the presence of vinblastine. Right panel: MCF-7/VP cells were treated as indicated above in the absence or presence of 1 nM vincristine. The MRP1 antagonism score is calculated as the percentage survival of cells in the absence of vincristine/percentage survival in the presence of vincristine. In both cases, a value of **1** indicates that the compound has no affect on drug sensitivity, while increasing values indicate increasing antagonism of the transport protein. Concentrations of compounds **1**−**5** above their IC_{50} toward MCF-7 cells are not indicated. Data for one of three similar experiments are shown.

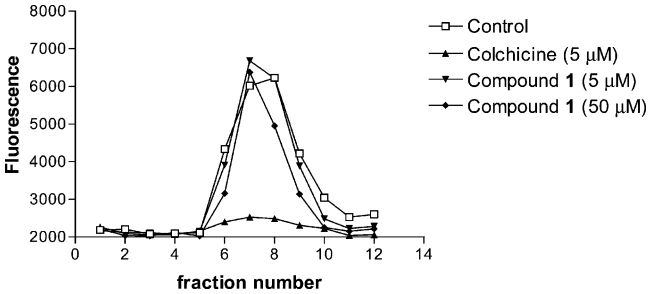

Figure 4. Competition for colchicine binding.

but enhance direct cytotoxicity. Thus, the 2-OMe-substituted compound **4** is most conducive to inhibition of Pgp for reversing Pgp-mediated resistance to vinblastine. Whether compound **1** also has this attribute cannot be determined due to its high cytotoxicity. However, because **1** at concentrations below its IC_{50} had no effect on Pgp-mediated resistance, it is possible that it is not a substrate for Pgp but does not inhibit Pgp like compounds **2**−**5**.

Effects of Compound 1 on Colchicine and Vinblastine Binding to Tubulin. Colchicine Binding. The ability of **1** to compete with colchicine for binding to bovine brain tubulin was assessed using a fluorescent colchicine analog (Figure 4). The colchicine analog was incubated with tubulin either alone or in the presence of 5 μM unlabeled colchicine or 5 or 50 μM **1**. Samples were then subjected to gel filtration chromatography on Sephadex G-25 (Superfine) equilibrated with binding buffer, and 0.5 mL fractions were collected and analyzed for fluorescence (excitation = 485 nm, emission = 535 nm).

Fluorescent colchicine that is bound to tubulin eluted in fractions 6−10, whereas unbound ligand eluted in fractions 16−24. As indicated in Figure 4, inclusion of unlabeled colchicine in the incubation competed off approximately 90% of the fluorescent colchicine. In contrast, neither concentration of **1** affected the binding of fluorescent colchicine to tubulin indicating that **1** does not bind at the colchicine binding site of tubulin.

Vinblastine Binding. Incubation of cells with high concentrations of vinblastine causes the formation of paracrystals of tubulin. We have previously used this phenomenon to demonstrate that compounds that interact with the vinblastine binding site of tubulin, for example, rhizoxin and cryptophycin, prevent the formation of these paracrystals.[45] The effects of **1** on vinblastine-tubulin paracrystal formation in aortic smooth muscle cells (A-10) were examined. As demonstrated in Figure 5, these cells have dense, well-organized microtubules and an elongated morphology (panel A). Treatment of the cells with 10 μM **1** caused pronounced depolymerization of the microtubules (panel B). Vinblastine (5 μM) also caused the loss of microtubules but, as expected, promoted the formation of numerous vinblastine-tubulin paracrystals in the cells (panel C). Pretreatment of the cells with 10 μM **1** did not prevent paracrystals formation (panel D), indicating that this compound does not interfere with the vinblastine binding site on tubulin.

Effects of 1 on Assembly of Bovine Brain Tubulin (Figure 6). Purified tubulin was incubated at 4 °C with ethanol (as a solvent control, 5 μM colchicine, 5 μM paclitaxel, 5 μM **1**, or 5 μM **1** plus 5 μM paclitaxel. GTP was added and samples were incubated at 37 °C for the indicated times.

Colchicine (the positive control) strongly suppressed tubulin assembly, while **1** caused a moderate reduction in the rate of tubulin polymerization. As expected, paclitaxel promoted the assembly of tubulin, and this effect was not inhibited by **1**. These results indicate that **1** directly interacts with tubulin, albeit with lower affinity and/or efficacy than colchicine and does not interfere with paclitaxel-promoted assembly of tubulin.

Further Effects of 1 on Assembly of Bovine Brain Tubulin. Figure 7, left panel: Purified tubulin (67 μM) was incubated at 4 °C with EtOH (as a solvent control), colchicine (5 μM), or **1** (2, 5, 10 or 20 μM). GTP was added and the samples were incubated at 37 °C for the indicated times, while the absorbance of 340 nm was monitored. In this assay, the IC_{50} is approximately 20 μM (noting that the tubulin concentration in the assay is 67 μM, indicating that it is a substoichiometric inhibitor of microtubule assembly). Figure 7, right panel: As before, colchicine (the positive control) strongly suppressed tubulin assembly. Compound **1** caused a dose-dependent reduction in both the rate and the extent of tubulin polymerization. Purified tubulin was incubated at 4 °C with EtOH, with paclitaxel (5 μM) alone, or in the presence of **1** (2, 5, 10, or 20 μM). GTP was added, and the samples were incubated at 37 °C for the indicated times while the absorbance of 340 nm was monitored. As before, paclitaxel promoted the assembly of tubulin (manifested as the loss of the lag time for the initiation

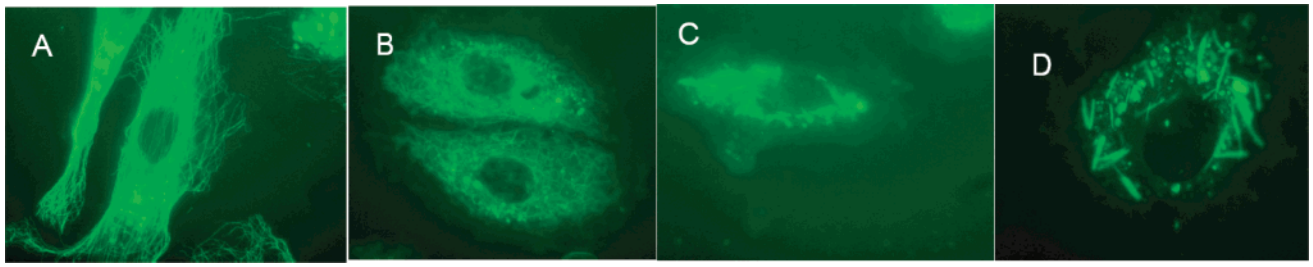

Figure 5. Tubulin paracrystal formation with vinblastin with and without compound **1**.

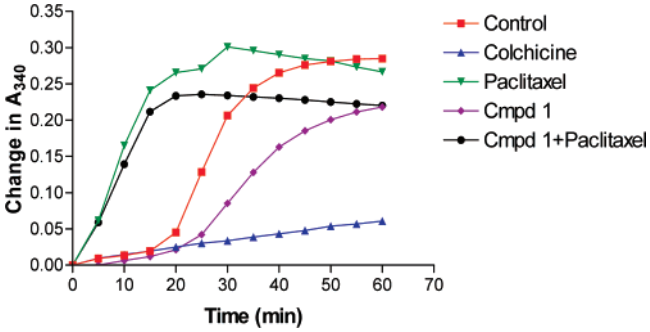

Figure 6. Effect of **1** on the assembly of bovine brain tubulin.

of polymerization), and this effect was not inhibited by **1** at concentrations up to at least 20 μM. Compound **1** did cause dose-dependent reductions in the maximal extent of tubulin polymerization, which is consistent with its ability to bind to tubulin monomers. Thus, compound **1** directly interacts with tubulin monomers, albeit with lower affinity and/or efficacy than colchicine. This is independent of the paclitaxel binding site and, from the previous binding experiments (Figures 4 and 5), also is independent of the vinblastine and colchicine binding sites. Thus, compound **1** has a different binding site on tubulin.

In addition to the sensitization assay shown in Figure 3, the compounds were evaluated in a drug-accumulation assay in which their abilities to increase the uptake of [^{3}H]vinblastine into NCI/ADR cells was determined according to the following protocol. NCI/ADR cells were plated into 24-well tissue culture dishes and allowed to grow to 90% confluency. The cells were washed with PBS and then incubated in 0.5 mL of RPMI 1640 medium containing the test compound and 20 nM [^{3}H]-vinblastine sulfate (10−15 Ci/mmole) for 60 min at 37 °C. The cultures were rapidly washed three times with ice-cold PBS. Intracellular [^{3}H]vinblastine was solubilized with 0.3 mL of 1% sodium dodecylsulfate in PBS and quantified by liquid scintillation counting.

The data for verapamil and compound **4** are shown in Figure 8. Compound **4** is of similar potency but more efficacious than verapamil. The ability of compound **4** to inhibit Pgp activity was confirmed in studies that demonstrated dose-dependent increases in the intracellular accumulation of [^{3}H]vinblastine by NCI/ADR cells with potency similar to that of verapamil (Figure 8).

In summary, we synthesized and evaluated a series of 7-benzyl-4-methyl-5-[(2-substituted phenyl)ethyl]-7*H*-pyrrolo-[2,3-*d*]pyrimidin-2-amines **1**−**5** and their 7-desbenzyl analogs **6**−**10** (Figure 1). We have determined that compounds **1**−**5** are antitumor agents and antimitotic agents that cause a dose−dependent depletion of microtubules in intact cells. Studies indicate that they do not bind to the colchicine or Vinca or paclitaxel binding sites and inhibit tumor cell lines that are both sensitive and resistant (Pgp or MRP1) to clinically used antimitotic drugs. We have confirmed that compound **1** does indeed bind to tubulin at a site different from the colchicine, Vinca, or paclitaxel binding sites. In addition, compounds **2**−**5** restore sensitivity of a Pgp expressing tumor cell line to antimitotic agents. Compound **1**, the most potent analog, inhibited all of the NCIs 60 tumor cell lines with GI_{50}s at nanomolar to submicromolar levels. Thus, compounds in this series **1**−**5** demonstrated important attributes as potential antitumor agents and/or Pgp inhibitory agents to be used alone or in combination with other chemotherapeutic agents (including antimitotic agents) against sensitive as well as resistant tumors.

Experimental Section

General Methods for Biological Evaluations. Materials: MCF-7 breast carcinoma cells and NCI/ADR cells, an MDR line that overexpresses Pgp, were obtained from the Division of Cancer Treatment of the National Cancer Institute. MCF-7/VP cells that express MRP1 but not Pgp were provided by Drs. Schneider and Cowan.[46] Human bladder carcinoma T24 cells were from the American Type Culture Collection. Sulforhodamine B, antibodies against β-tubulin (T-4026), proteinase K (P2308), RNase A (R-5503), and actomyosin (A-6394) were obtained from Sigma Chemical Company (St. Louis, MO). RPMI-1640 and α-MEM culture media and fetal bovine serum were from GibcoBRL (Grand Island, NY).

Assay of Cytotoxicity and Reversals of MDR: To test for reversal of Pgp-mediated MDR, NCI/ADR cells were placed into 96-well tissue culture plates at approximately 15% confluency and allowed to attach and recover for 24 h. The cells were then treated with varying concentrations (as allowed by solubility) of a test compound in the presence of 0 or 50 nM vinblastine for 48 h according to previously described procedures.[47−53] After 48 h, cell survival was assayed using the sulforhodamine B (SRB) binding assay.[54] The percentage of cells killed is calculated as the percentage decrease in SRB binding as compared with control cultures and is taken from the mean of the absorbance measurements of three equally treated wells. Reversal of MDR is indicated if the compound enhances the toxicity of vinblastine toward the NCI/ADR cells. The reversal index (Pgp Antagonism Score) is calculated as the percentage of surviving NCI/ADR cells in the absence of vinblastine/the percentage of surviving NCI/ADR cells in the presence of vinblastine. Control cultures included equivalent amounts of ethanol (as the solvent control), which does not modulate the growth or drug-sensitivity of these cells at the doses used in these studies. To assess the toxicity of the compounds toward drug-sensitive cells, the effects of the test modulators on the growth of drug-sensitive MCF-7 cells were determined by the same methods. To test for reversal of MRP1-mediated MDR, MCF-7/VP cells were placed into 96-well tissue culture plates at approximately 15% confluency and were allowed to attach and recover for 24 h. The cells were then treated with varying concentrations (as allowed by solubility) of a test compound in the presence of 0 or 1 nM vincristine for 48 h as above. After 48 h, cell survival was assayed using the SRB binding assay. Reversal of MDR is indicated if the compound enhances the toxicity of vincristine toward the MCF-7/VP cells. The reversal index (MRP1 Antagonism Score) is calculated as the percentage of surviving MCF-7/VP cells in the absence of vincristine/the percentage of surviving MCF-7/VP cells in the presence of vincristine.

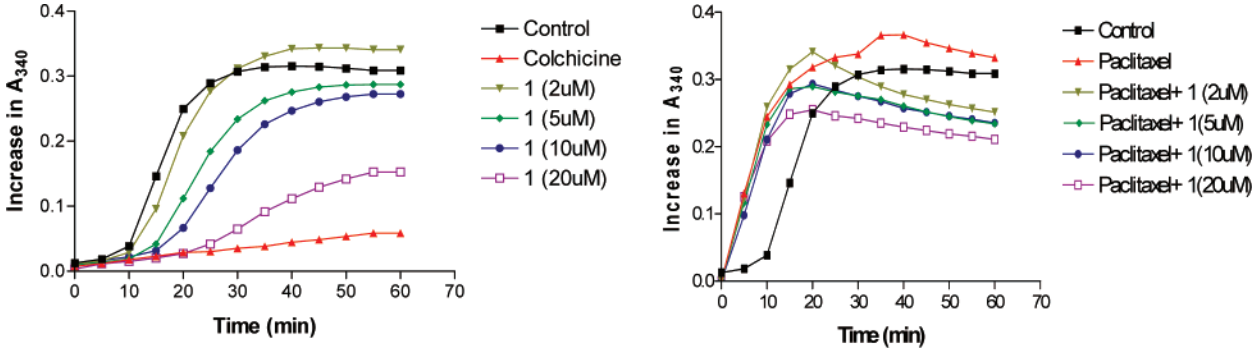

Figure 7. Further effects of **1** on bovine brain tubulin.

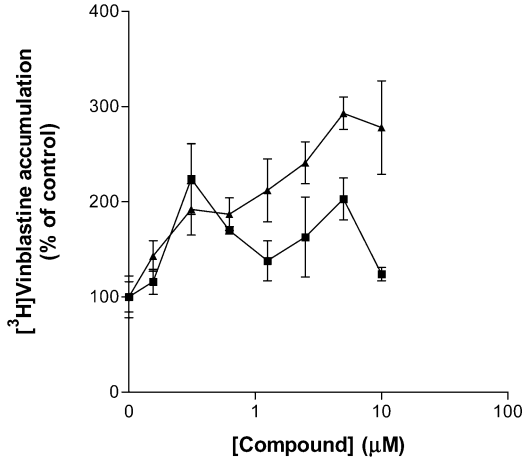

Figure 8. [^{3}H] Vinblastine accumulation assay for verapamil (■) and compound **4** (▲).

Cell Cycle Analyses: HL-60 cells were treated with ethanol, paclitaxel, vinblastine, colchicine, or compound **1** for 24 or 48 h, and DNA was stained by a procedure similar to that of Vindelov et al.[55] Briefly, cells were harvested by centrifugation, resuspended in citrate buffer (250 mM sucrose, 40 mM trisodium citrate, pH 7.6, and 5% dimethylsulfoxide) to a concentration of 5×10^5 cells/200 μL, and mixed with 1.8 mL of trypsin (0.03 mg/mL) in staining buffer (3.4 mM trisodium citrate, 0.5 mM Tris, pH 7.6, 0.1% NP-40, and 1.5 mM spermine) for 10 min. To each sample, 1.5 mL of trypsin inhibitor (0.5 mg/mL) and RNase A (0.1 mg/mL) in staining buffer were added for 10 min, followed by 1.5 mL of propidium iodide (0.4 mg/mL) and spermine (1.2 mg/mL) in staining buffer. After 30 min at 4 °C, samples were filtered through 30 μm nylon mesh, centrifuged at $721 \times g$ for 5 min and resuspended in 1 mL of staining buffer. The DNA contents of the cells were measured using a Beckton Dickinson FACScan Flow Cytometer, and cell cycle distribution was analyzed using the program MacCycle.

Cytoskeleton Staining: A-10 rat smooth muscle cells were grown to near confluency on glass cover slips and treated with the indicated compounds for 24 h. Microtubules were stained with monoclonal anti-β-tubulin and visualized with fluorescein-conjugated anti-mouse IgG. For staining of microfilaments, cells were fixed with 3% *p*-formaldehyde, permeabilized with 0.2% Triton X-100, and reduced with sodium borohydride (1 mg/mL). Microfilaments were visualized by incubation with 100 nM of TRITC-phalloidin for 45 min at 37 °C. Microtubules and microfilaments were imaged using a Nikon Optiphot-2 microscope with a Bio-Rad MRC 600 Confocal Laser Scanning system. The images were reconstructed using VoxelView Ultra Software and were printed on a Kodak Model XL 7700 digital continuous tone printer.

In Vitro Tubulin Experiments. Microtubule protein (MTP), comprising tubulin and MAPs, was isolated from fresh bovine brain by three cycles of assembly and disassembly, and pure tubulin was isolated by subsequent ion-exchange chromatography, as described by Vallee.[56] The effects of compound **1** on tubulin assembly were determined following the procedures of Bai et al.[57] Briefly, 0.25 mL samples containing 2.5 mg of tubulin/mL (67 μM tubulin) in 1 M glutamate, pH 6.6, containing 4% DMSO were incubated with ethanol, compound **1**, paclitaxel, or colchicine at 0 °C for 15 min. GTP (0.5 mM) was then added to the samples followed by rapid warming to 37 °C, and the absorbance at 340 nm was continuously monitored for approximately 60 min. Microtubule assembly is measured as increasing A_{340} due to light scattering by the polymers. Interaction of Compound **1** with the colchicine-binding site of tubulin was examined using the competition assay kit from Cytoskeleton, Inc. (Denver, CO), in which purified tubulin was incubated with compound **1** or unlabeled colchicine and fluorescently labeled colchicine for 30 min at 37 °C. The samples were then transferred to a column of Sephadex G-25, and 0.5 mL fractions were collected and analyzed for fluorescence intensity with an excitation wavelength of 485 nm and an emission wavelength of 535 nm. In this assay, colchicine or a compound interacting at the same site displaces the fluorescent colchicine that elutes at the void volume of the column.

[^{3}H]Vinblastine Accumulation Assay. NCI/ADR cells were plated into 24-well tissue culture dishes and allowed to grow to 90% confluency. The cells were washed with PBS and then incubated in 0.5 mL of RPMI 1640 medium containing the test compound and 20 nM [^{3}H]vinblastine sulfate (10−15 Ci/mmole) for 60 min at 37 °C. The cultures were rapidly washed three times with ice-cold PBS. Intracellular [^{3}H]vinblastine was solubilized with 0.3 mL of 1% sodium dodecylsulfate in PBS and quantified by liquid scintillation counting.

General Methods for Synthesis. All evaporations were carried out in vacuo with a rotary evaporator. Analytical samples were dried in vacuo (0.2 mmHg) in an Abderhalden drying apparatus over P_2O_5 and ethanol by reflux. Thin layer chromatography (TLC) was performed on silica gel plates with fluorescent indicator. Spots were visualized by UV light (254 and 365 nm). All analytical samples were homogeneous on TLC in at least two different solvent systems. Purification by column and flash chromatography was carried out using Merck silica gel 60 (200−400 mesh). The amount (weight) of silica gel for column chromatography was in the range of 50−100 times the amount (weight) of the crude compounds being separated. Columns were dry packed unless specified otherwise. Solvent systems are reported as volume percent mixture. Melting points were determined on a Mel-Temp II melting point apparatus and are uncorrected. Proton nuclear magnetic resonance (^{1}H NMR) spectra were recorded on a Bruker WH-300 (300 MHz) spectrometer. The chemical shift (δ) values are reported as parts per million (ppm) relative to tetramethylsilane as internal standard; s = singlet, d = doublet, t = triplet, q = quartet, m = multiplet, bs = broad singlet, exch = protons exchangeable by addition of D_2O. Elemental analyses were performed by Atlantic Microlab, Inc., Norcross, GA. Elemental compositions were within ± 0.4% of the calculated values. Fractional moles of water or organic solvents frequently found in some analytic samples could not be removed despite 24 h of drying in vacuo and were confirmed, where possible, by their presence in the ^{1}H NMR spectrum. All solvents and chemicals were purchased from Aldrich Chemical Co. and Fisher Scientific and

were used as received, except anhydrous solvents, which were freshly dried in the laboratory.

General Procedure for the Synthesis of 12a−d. To a 25-mL round-bottom flask protected from light with aluminum foil were added **11**,[40] the appropriate (substituted) iodobenzene, copper(I) iodide, and tetrakis(triphenylphosphine)-palladium(0) dissolved in anhydrous dichloroethane, followed by the addition of triethylamine. The resulting, dark brown, solution was stirred at room temperature under nitrogen for 3.5 h. Then CH_2Cl_2 (50 mL) was added to the solution, and the reaction mixture was washed with brine (20 mL × 2), and the organic layer was separated and dried over Na_2SO_4 and filtered. The filtrate was evaporated in vacuo. To this residue was added silica gel (10 g) and methanol (20 mL), and the solvent was evaporated to afford a plug. The silica gel plug obtained was loaded onto a silica gel column and eluted with 1:1:7 ethyl acetate/triethylamine/hexanes. Fractions containing the product (TLC) were pooled, and the solvent was evaporated to afford analytically pure compound.

***N*-{7-Benzyl-4-methyl-5-[(3,4,5-trimethoxyphenyl)ethynyl]-7*H*-pyrrolo[2,3-*d*]pyrimidin-2-yl}-2,2-dimethylpropanamide (12a).** Compound **12a** was synthesized from **11** (0.30 g, 0.88 mmol), 5-iodo-1,2,3-trimethoxybenzene (0.32 g, 1.10 mmol), copper(I) iodide (0.01 g, 0.17 mmol), tetrakis(triphenylphosphine)-palladium-(0) (0.13 g, 0.07 mmol), and triethylamine (0.2 mL) using the general procedure described above to afford after purification 0.36 g (79%) as a white solid: TLC R_f 0.24 (ethyl acetate/triethylamine/hexanes, 1:1:3); mp 130−133 °C; ^{1}H NMR (DMSO-d_6) δ 1.24 (s, 9 H, C(CH$_3$)$_3$), 2.85 (s, 3 H, 4-CH$_3$), 3.68 (s, 3 H, 4′-OCH$_3$), 3.80 (s, 6 H, 3′ & 5′-OCH$_3$), 5.39 (s, 2 H, C*H*$_2$C$_6$H$_5$), 6.82 (s, 2 H, C$_6$H$_2$), 7.31−7.35 (m, 5 H, C$_6$H$_5$), 7.90 (s, 1 H, 6-H), 9.91 (s, 1 H, 2-N*H*Piv, exch). Anal. (C$_{30}$H$_{32}$N$_4$O$_4$) C, H, N.

***N*-{7-Benzyl-4-methyl-5-[(4-methoxyphenyl)ethynyl]-7*H*-pyrrolo[2,3-*d*]pyrimidin-2-yl}-2,2-dimethylpropanamide (12b).** Compound **12b** was synthesized from **11** (0.34 g, 1.11 mmol), 1-iodo-4-methoxybenzene (0.29 g, 1.23 mmol), copper(I) iodide (0.01 g, 0.07 mmol), tetrakis(triphenylphosphine) palladium(0) (0.12 g, 0.10 mmol), and triethylamine (0.3 mL) using the general procedure described above to afford after purification 0.79 g (53%) as a pale yellow solid: TLC R_f 0.32 (ethyl acetate/triethylamine/hexanes, 1:1:3); mp 158−160 °C; ^{1}H NMR (DMSO-d_6) δ 1.24 (s, 9 H, C(CH$_3$)$_3$), 2.84 (s, 3 H, 4-CH$_3$), 3.79 (s, 3 H, OCH$_3$), 5.39 (s, 2 H, C*H*$_2$C$_6$H$_5$), 6.96 (d, 2 H, J = 8.7 Hz, C$_6$H$_4$), 7.27 (m, 4 H, C$_6$H$_5$), 7.44 (d, 2 H, J = 7.8 Hz, C$_6$H$_4$), 7.62 (m, 1 H, C$_6$H$_5$), 7.87 (s, 1 H, 6-H), 9.89 (s, 1 H, 2-N*H*Piv, exch). Anal. (C$_{28}$H$_{28}$N$_4$O$_2$·0.1H$_2$O) C, H, N.

***N*-{7-Benzyl-4-methyl-5-[(3-methoxyphenyl)ethynyl]-7*H*-pyrrolo[2,3-*d*]pyrimidin-2-yl}-2,2-dimethylpropanamide (12c).** Compound **12c** was synthesized from **11** (0.91 g, 2.6 mmol), 1-iodo-3-methoxybenzene (0.77 g, 3.30 mmol), copper(I) iodide (0.04 g, 0.20 mmol), tetrakis(triphenylphosphine) palladium(0) (0.36 g, 0.30 mmol), and triethylamine (0.3 mL) using the general procedure described above to afford after purification 0.74 g (62%) as a pale yellow solid: TLC R_f 0.27 (ethyl acetate/triethylamine/hexanes, 1:1:3); mp 110−112 °C; ^{1}H NMR (DMSO-d_6) δ 1.24 (s, 9 H, C(CH$_3$)$_3$), 2.85 (s, 3 H, 4-CH$_3$), 3.78 (s, 3 H, OCH$_3$), 5.39 (s, 2 H, C*H*$_2$C$_6$H$_5$), 6.96−7.11 (m, 3 H, C$_6$H$_4$), 7.32 (m, 6 H, C$_6$H$_5$ & C$_6$H$_4$), 7.93 (s, 1 H, 6-H), 9.90 (s, 1 H, 2-N*H*Piv, exch). Anal. (C$_{28}$H$_{28}$N$_4$O$_2$·0.1MeOH) C, H. N.

***N*-{7-Benzyl-4-methyl-5-[(2-methoxyphenyl)ethynyl]-7*H*-pyrrolo[2,3-*d*]pyrimidin-2-yl}-2,2-dimethylpropanamide (12d).** Compound **12d** was synthesized from **11** (0.87 g, 2.50 mmol), 1-iodo-2-methoxybenzene (0.64 g, 2.75 mmol), copper(I) iodide (0.03 g, 0.17 mmol), tetrakis(triphenylphosphine) palladium(0) (0.12 g, 0.10 mmol), and triethylamine (0.3 mL) using the general procedure described above to afford after purification 0.54 g (48%) as a pale yellow solid: TLC R_f 0.23 (ethyl acetate/triethylamine/hexanes, 1:1:3); mp 153−155.5 °C; ^{1}H NMR (DMSO-d_6) δ 1.24 (s, 9 H, C(CH$_3$)$_3$), 2.88 (s, 3 H, 4-CH$_3$), 3.85 (s, 3 H, OCH$_3$), 5.39 (s, 2 H, C*H*$_2$C$_6$H$_5$), 6.97 (t, 1 H, C$_6$H$_5$), 7.09 (d, 1 H, J = 8.3 Hz, C$_6$H$_5$), 7.35 (m, 6 H, C$_6$H$_5$ & C$_6$H$_4$), 7.45 (d, 1 H, J = 6.0 Hz, C$_6$H$_4$), 7.90 (s, 1 H, 6-H), 9.91 (s, 1 H, 2-N*H*Piv, exch). Anal. (C$_{28}$H$_{28}$N$_4$O$_2$) C, H, N.

General Procedure for the Synthesis of 13a−d. To a Parr hydrogenation bottle was added **12a−d** dissolved in dichloromethane (20 mL) and methanol (20 mL), followed by the addition of 5% Pd/C. The mixture was hydrogenated at 50 psi at room temperature overnight. After filtration, the catalyst was thoroughly washed with hot methanol (20 mL × 3). The filtrate was concentrated in vacuo and silica gel (10 g) and methanol (20 mL) were added to the residue. The solvent was evaporated to afford a plug. The silica gel plug obtained was loaded onto a silica gel column and eluted with 1:1:7 ethyl acetate/triethylamine/hexanes. Fractions containing the product (TLC) were pooled, and the solvent was evaporated to afford analytically pure compound.

***N*-{7-Benzyl-5-[2-(3,4,5-trimethoxyphenyl)ethyl]-4-methyl-7*H*-pyrrolo[2,3-*d*]pyrimidin-2-yl}-2,2-dimethylpropanamide (13a).** Compound **13a** was synthesized from **12a** (0.70 g, 1.37 mmol) and 5% Pd/C (0.50 g) using the general procedure described above to afford 0.53 g (75%) as a sticky solid: TLC R_f 0.24 (ethyl acetate/triethylamine/hexanes, 1:1:3); ^{1}H NMR (DMSO-d_6) δ 1.23 (s, 9 H, C(CH$_3$)$_3$), 2.70 (s, 3 H, 4-CH$_3$), 2.86 (t, 2 H, J = 7.4 Hz, C*H*$_2$-CH$_2$), 3.07 (t, 2 H, J = 7.4 Hz, CH$_2$C*H*$_2$), 3.69 (s, 3 H, 4′-OCH$_3$), 3.82 (s, 6 H, 3′- and 5′-OCH$_3$), 5.32 (s, 2 H, C*H*$_2$C$_6$H$_5$), 6.53 (s, 1 H, 6-H), 7.21−7.30 (m, 7 H, C$_6$H$_5$ and C$_6$H$_2$), 9.73 (s, 1 H, 2-N*H*Piv, exch). Anal. (C$_{30}$H$_{36}$N$_4$O$_4$) C, H, N.

***N*-{7-Benzyl-5-[2-(4-methoxyphenyl)ethyl]-4-methyl-7*H*-pyrrolo[2,3-*d*]pyrimidin-2-yl}-2,2-dimethylpropanamide (13b).** Compound **13b** was synthesized from **12b** (0.70 g, 1.57 mmol) and 5% Pd/C (0.50 g) using the general procedure described above to afford 0.47 g (67%) as a white foam: TLC R_f 0.42 (ethyl acetate/triethylamine/hexanes, 1:1:3); ^{1}H NMR (DMSO-d_6) δ 1.23 (s, 9 H, C(CH$_3$)$_3$), 2.69 (s, 3 H, CH$_3$), 2.84 (t, 2 H, J = 7.9 Hz, CH$_2$-CH$_2$), 3.02 (t, 2 H, J = 7.9 Hz, CH$_2$CH$_2$), 3.70 (s, 3 H, OCH$_3$), 5.31 (s, 2 H, C*H*$_2$C$_6$H$_5$), 6.82 (d, 2 H, J = 8.4 Hz, C$_6$H$_4$), 6.90−7.62 (m, 8 H, C$_6$H$_5$, C$_6$H$_4$, and 6-H), 9.95 (s, 1 H, 2-N*H*Piv, exch). Anal. (C$_{28}$H$_{32}$N$_4$O$_2$) C, H, N.

***N*-{7-Benzyl-5-[2-(3-methoxyphenyl)ethyl]-4-methyl-7*H*-pyrrolo[2,3-*d*]pyrimidin-2-yl}-2,2-dimethylpropanamide (13c).** Compound **13c** was synthesized from **12c** (0.74 g, 1.60 mmol) and 5% Pd/C (0.50 g) using the general procedure described above to afford 0.50 g (68%) as a sticky solid: TLC R_f 0.41 (ethyl acetate/triethylamine/hexanes, 1:1:3); ^{1}H NMR (DMSO-d_6) δ 1.21 (s, 9 H, C(CH$_3$)$_3$), 2.40 (s, 3 H, 4-CH$_3$), 2.87 (t, 2 H, J = 7.1 Hz, C*H*$_2$-CH$_2$), 3.04 (t, 2 H, J = 7.1 Hz, CH$_2$C*H*$_2$), 3.70 (s, 3 H, OCH$_3$), 6.77−7.31 (m, 10 H, C$_6$H$_5$, C$_6$H$_4$, and 6-H), 9.73 (s, 1 H, 2-N*H*Piv, exch). Anal. (C$_{28}$H$_{32}$N$_4$O$_2$·0.1MeOH) C, H, N.

***N*-{7-Benzyl-5-[2-(2-methoxyphenyl)ethyl]-4-methyl-7*H*-pyrrolo[2,3-*d*]pyrimidin-2-yl}-2,2-dimethylpropanamide (13d).** Compound **13d** was synthesized from **12d** (0.50 g, 1.10 mmol) and 5% Pd/C (0.60 g) using the general procedure described above to afford 0.46 g (91%) as an oil: TLC R_f 0.42 (ethyl acetate/triethylamine/hexanes, 1:1:3); ^{1}H NMR (DMSO-d_6) δ 1.23 (s, 9 H, C(CH$_3$)$_3$), 2.71 (s, 3 H, 4-CH$_3$), 2.86 (t, 2 H, J = 8.0 Hz, C*H*$_2$CH$_2$), 2.97 (t, 2 H, J = 8.0 Hz, CH$_2$C*H*$_2$), 3.75 (s, 3 H, OCH$_3$), 5.32 (s, 2 H, C*H*$_2$C$_6$H$_5$), 6.83−7.34 (m, 10 H, C$_6$H$_5$, C$_6$H$_4$, and 6-H), 9.72 (s, 1 H, 2-N*H*Piv, exch). When placed in a vial, the oil solidifies. Anal. (C$_{28}$H$_{32}$N$_4$O$_2$·0.1H$_2$O) C, H, N.

General Procedure for the Synthesis of 1−4. To a round-bottom flask was added **13a−d** dissolved in methanol (10 mL), followed by the addition of 1 N NaOH (2 mL). The reaction mixture was heated at reflux at 80 °C for 24 h. The reaction was then cooled and the MeOH evaporated under vacuum. The precipitated solid obtained was filtered, washed with cold water and a mixture of 1:2 ethyl acetate/hexanes, and dried to afford analytically pure compound.

7-Benzyl-4-methyl-5-[2-(3,4,5-trimethoxyphenyl)ethyl]-7*H*-pyrrolo[2,3-*d*]pyrimidin-2-amine (1). Compound **1** was synthesized from **13a** (0.46 g, 0.89 mmol) using the general procedure described above to afford 0.33 g (86%) as a pale yellow solid: TLC R_f 0.40 (ethyl acetate/triethylamine/hexanes, 5:1:3); mp 168.5−

171 °C; ^{1}H NMR (DMSO-d_6) δ 2.52 (s, 3 H, 4-CH_3), 2.84 (t, 2 H, J = 8.0 Hz, CH_2CH_2), 3.00 (t, 2 H, J = 8.0 Hz, CH_2CH_2), 3.70 (s, 3 H, 4′-OCH_3), 3.81 (s, 6 H, 3′- and 5′-OCH_3), 5.17 (s, 2 H, $CH_2C_6H_5$), 6.08 (s, 2 H, 2-NH_2, exch), 6.52 (s, 2H, C_6H_2), 7.09 (s, 1 H, 6-H), 7.27 (m, 5 H, C_6H_5). Anal. ($C_{25}H_{28}N_4O_3$) C, H, N.

7-Benzyl-5-[2-(4-methoxyphenyl)ethyl]-4-methyl-7*H*-pyrrolo-[2,3-*d*]pyrimidin-2-amine (2). Compound **2** was synthesized from **13b** (0.45 g, 0.98 mmol) using the general procedure described above to afford 0.29 g (79%) as a white solid: TLC R_f 0.34 (ethyl acetate/triethylamine/hexanes, 5:1:3); mp 153−156 °C; ^{1}H NMR (DMSO-d_6) δ 2.53 (s, 3 H, 4-CH_3), 2.81 (t, 2 H, CH_2CH_2), 2.90 (t, 2 H, CH_2CH_2), 3.71 (s, 3 H, OCH_3), 5.16 (s, 2 H, $CH_2C_6H_5$), 6.07 (s, 2 H, 2-NH_2, exch), 6.74 (s, 1 H, 6-H), 6.83 (d, 2 H, J = 8.6 Hz, C_6H_4), 7.08−7.32 (m, 7 H, C_6H_5 and C_6H_4). Anal. ($C_{23}H_{24}N_4O$·0.25CH_3-$COOCH_2CH_3$) C, H, N.

7-Benzyl-5-[2-(3-methoxyphenyl)ethyl]-4-methyl-7*H*-pyrrolo-[2,3-*d*]pyrimidin-2-amine (3). Compound **3** was synthesized from **13c** (0.45 g, 0.98 mmol) using the general procedure described above to afford 0.32 g (87%) as a white solid: TLC R_f 0.46 (ethyl acetate/triethylamine/hexanes, 5:1:3); mp 126−127.5 °C; ^{1}H NMR (DMSO-d_6) δ 2.53 (s, 3 H, 4-CH_3), 2.85 (t, 2 H, J = 8.0 Hz, CH_2-CH_2), 2.97 (t, 2 H, J = 8.0 Hz, CH_2CH_2), 3.70 (s, 3 H, OCH_3), 5.17 (s, 2 H, $CH_2C_6H_5$), 6.08 (s, 2 H, 2-NH_2, exch), 6.73−7.31 (m, 10 H, C_6H_5, C_6H_4, and 6-H). Anal. ($C_{23}H_{24}N_4O$·0.10MeOH) C, H, N.

7-Benzyl-5-[2-(2-methoxyphenyl)ethyl]-4-methyl-7*H*-pyrrolo-[2,3-*d*]pyrimidin-2-amine (4). Compound **4** was synthesized from **13d** (0.40 g, 0.88 mmol) using the general procedure described above to afford 0.29 g (90%) as a pale pink solid: TLC R_f 0.50 (ethyl acetate/triethylamine/hexanes, 5:1:3); mp 138.5−140 °C; ^{1}H NMR (DMSO-d_6) δ 2.50 (s, 3 H, 4-CH_3), 2.85−2.91 (m, 4 H, CH_2-CH_2), 3.76 (s, 3 H, OCH_3), 5.17 (s, 2 H, $CH_2C_6H_5$), 6.08 (s, 2 H, 2-NH_2, exch), 6.78−7.32 (m, 9H, C_6H_5 and C_6H_4). Anal. ($C_{23}H_{24}N_4O$) C, H, N.

General Procedure for the Synthesis of 6−9. To a 25-mL round-bottom flask cooled to −78 °C were added **1**−**4** and liquid NH_3 (20 mL), followed by the addition of sodium metal (one and one-half the weight of **1**−**4**). The reaction was maintained at −78 °C for 4.5 h and then quenched with NH_4Cl (same as the weight of **1**−**4**). The mixture was allowed to warm to room temperature and the liquid NH_3 was evaporated. The residue was purified by column chromatography on silica gel and eluted with 20:2:2:1 ethyl acetate/ethanol/acetone/water to afford analytically pure compound.

4-Methyl-5-[2-(3,4,5-trimethoxyphenyl)ethyl]-7*H*-pyrrolo[2,3-*d*]pyrimidin-2-amine (6). Compound **6** was synthesized from **1** (0.27 g, 0.63 mmol) using the general procedure described above to afford 0.06 g (28%) as a pale yellow solid: TLC R_f 0.33 (ethyl acetate/ethanol/acetone/water, 20:2:2:1); mp 175.8−178.8 °C; ^{1}H NMR (DMSO-d_6) δ 2.51 (s, 3 H, 4-CH_3), 2.79−2.96 (m, 4 H, CH_2-CH_2), 3.72 (s, 3 H, 4′-OCH_3), 3.81 (s, 6 H, 3′ & 5′-OCH_3), 5.89 (s, 2 H, NH_2, exch), 6.07 (s, 1 H, 6-H), 6.53 (s, 2 H, C_6H_2), 10.73 (s, 1 H, 7-NH, exch). Anal. ($C_{18}H_{22}N_4O_3$) C, H, N.

5-[2-(4-Methoxyphenyl)ethyl]-4-methyl-7*H*-pyrrolo[2,3-*d*]pyrimidin-2-amine (7). Compound **7** was synthesized from **2** (0.24 g, 0.68 mmol) using the general procedure described above to afford 0.05 g (28%) as a pale yellow power: TLC R_f 0.52 (ethyl acetate/ethanol/acetone/water, 20:2:2:1); mp 201−204.6 °C; ^{1}H NMR (DMSO-d_6) δ 2.50 (s, 3 H, 4-CH_3), 2.83−2.90 (m, 4 H, CH_2CH_2), 3.70 (s, 3 H, OCH_3), 5.89 (bs, 2 H, NH_2, exch), 6.66 (s, 1 H, 6-H), 6.81−6.84 (d, 2 H, J = 9.1 Hz, C_6H_4), 7.13−7.16 (d, 2 H, J = 9.1 Hz, C_6H_4), 10.71 (bs, 1 H, 7-NH, exch). Anal. ($C_{16}H_{18}N_4O$· 0.3MeOH) C, H, N.

5-[2-(3-Methoxyphenyl)ethyl]-4-methyl-7*H*-pyrrolo[2,3-*d*]pyrimidin-2-amine (8). Compound **8** was synthesized from **3** (0.20 g, 0.54 mmol) using the general procedure described above to afford 0.03 g (19%) as a pale yellow solid: TLC R_f 0.47 (ethyl acetate/ethanol/acetone/water, 20:2:2:1); mp 166−169 °C; ^{1}H NMR (DMSO-d_6) δ 2.49 (s, 3 H, 4-CH_3), 2.92 (m, 4 H, CH_2CH_2), 3.72 (s, 3 H, OCH_3), 5.87 (s, 2 H, NH_2, exch), 6.68−7.19 (m, 5 H, 6-H and C_6H_4), 10.71 (s, 1 H, 7-NH, exch). Anal. ($C_{16}H_{18}N_4O$) C, H, N.

5-[2-(2-Methoxyphenyl)ethyl]-4-methyl-7*H*-pyrrolo[2,3-*d*]pyrimidin-2-amine (9). Compound **9** was synthesized from **4** (0.22 g, 0.59 mmol) using the general procedure described above to afford 0.08 g (48%) as a white solid: TLC R_f 0.48 (ethyl acetate/ethanol/acetone/water, 20:2:2:1); mp 218.5−223 °C; ^{1}H NMR (DMSO-d_6) δ 2.52 (s, 3 H, 4-CH_3), 2.85 (s, 4 H, CH_2CH_2), 3.78 (s, 3 H, OCH_3), 5.88 (s, 2 H, NH_2, exch), 6.69 (s, 1 H, 6-H), 6.88 (t, 1 H, J = 7.2 Hz, C_6H_4), 6.96 (t, 1 H, J = 8.0 Hz, C_6H_4), 7.17 (m, 2 H, C_6H_4), 10.73 (s, 1 H, 7-NH, exch). Anal. ($C_{16}H_{18}N_4O$·0.2MeOH) C, H, N.

***N*-[7-Benzyl-4-methyl-5-(phenylethynyl)-7*H*-pyrrolo[2,3-*d*]pyrimidin-2-yl]-*N*-(2,2-dimethylpropanoyl)-2,2-dimethylpropanamide (15).** To a 50-mL round-bottom flask covered with aluminum foil were added **14**[40] (0.27 g, 0.42 mmol), ethynyl benzene (0.15 g, 1.5 mmol), copper(I) iodide (0.02 g, 0.1 mmol) and tetrakis-(triphenylphosphine)palladium(0) (0.06 g, 0.05 mmol) dissolved in anhydrous dichloroethane (5 mL) and triethylamine (0.14 mL). The resulting dark brown solution was stirred at room temperature under nitrogen for 24 h. The solvents were removed in vacuo, and the crude residue was flash chromatographed on silica gel and eluted with 1:1:10 ethyl acetate/triethylamine/hexanes to afford 0.20 g (78%) of **15** as a white solid: TLC R_f 0.45 (ethyl acetate/triethylamine/hexanes, 1:1:7); mp 125−127 °C; ^{1}H NMR (DMSO-d_6) δ 1.17 (s, 18 H, $C(CH_3)_3$), 2.90 (s, 3 H, 4-CH_3), 5.42 (s, 2 H, $CH_2C_6H_5$), 7.19−7.57 (m, 10 H, C_6H_5), 8.18 (s, 1 H, 6-H). Anal. ($C_{32}H_{34}N_4O_2$) C, H, N.

***N*-[7-Benzyl-4-methyl-5-(2-phenylethyl)-7*H*-pyrrolo[2,3-*d*]pyrimidin-2-yl]-*N*-(2,2-dimethylpropanoyl)-2,2-dimethylpropanamide (16).** To a Parr hydrogenation bottle was added **15** (0.27 g, 0.50 mmol) dissolved in CH_2Cl_2 (25 mL) and MeOH (25 mL), followed by the addition of 5% Pd/C (0.20 g). The mixture was then hydrogenated at 50 psi for 3.5 h. The catalyst was filtered and washed thoroughly with hot MeOH (20 mL), and the filtrate was evaporated in vacuo. The residue obtained was flash chromatographed on silica gel and eluted with 1:1:7 ethyl acetate/triethylamine/hexanes to afford 0.27 g (100%) of **16** as a white solid: TLC R_f 0.21 (ethyl acetate/triethylamine/hexanes, 1:1:7); mp 105.5−107 °C; ^{1}H NMR (DMSO-d_6) δ 1.15 (s, 18 H, $C(CH_3)_3$), 2.73 (s, 3 H, 4-CH_3), 2.93 (t, 2 H, J = 8.1 Hz, CH_2CH_2), 3.11 (t, 2 H, J = 8.1 Hz, CH_2CH_2), 5.33 (s, 2 H, $CH_2C_6H_5$), 7.09−7.31 (m, 10 H, C_6H_5), 7.42 (s, 1 H, 6-H). Anal. ($C_{32}H_{38}N_4O_2$) C, H, N.

7-Benzyl-4-methyl-5-(2-phenylethyl)-7*H*-pyrrolo[2,3-*d*]pyrimidin-2-amine (5). To a round-bottom flask was added **16** (0.23 g, mmol) suspended in MeOH (10 mL) and 1 N NaOH (5 mL). The reaction mixture was heated at reflux at 80 °C for 24 h. The reaction was cooled and the MeOH evaporated under vacuum. The precipitated solid was filtered, washed with cold water, and dried to afford 0.11 g (79%) of **5** as a white solid: TLC R_f 0.37 (ethyl acetate/triethylamine/hexanes, 5:1:3); mp 121.5−123 °C; ^{1}H NMR (DMSO-d_6) δ 2.54 (s, 3 H, 4-CH_3), 2.88−2.97 (m, 4 H, CH_2-CH_2), 5.17 (s, 2 H, CH_2Ph), 6.09 (s, 2 H, 2-NH_2, exch), 6.77 (s, 1 H, 6-H), 7.08−7.30 (m, 10 H, C_6H_5). Anal. ($C_{22}H_{22}N_4$·0.3H_2O) C, H, N.

4-Methyl-5-(2-phenylethyl)-7*H*-pyrrolo[2,3-*d*]pyrimidin-2-amine (10). To a 25-mL round-bottom flask cooled to −78 °C were added **5** (0.24 g, 0.70 mmol) and liquid NH_3 (20 mL), followed by the addition of sodium metal (0.18 g). The reaction was maintained at −78 °C for 4.5 h and then quenched with NH_4Cl (0.30 g). The mixture was allowed to warm to room temperature, and the liquid NH_3 was evaporated. The residue was purified by column chromatography on silica gel and eluted with 20:2:2:1 ethyl acetate/ethanol/acetone/water to afford 0.05 g (30%) of **10** as a pale yellow solid: TLC R_f 0.45 (ethyl acetate/ethanol/acetone/water, 20:2:2:1); mp 202.5−206 °C; ^{1}H NMR (DMSO-d_6) δ 2.50 (s, 3 H, CH_3), 2.88−2.97 (m, 4 H, CH_2CH_2), 5.88 (s, 2 H, NH_2, exch), 6.67 (s, 1 H, 6-H), 7.16−7.27 (m, 5 H, C_6H_5), 10.72 (s, 1 H, 7-NH, exch). Anal. ($C_{15}H_{16}N_4$·0.1H_2O) C, H, N.

Acknowledgment. This work was supported, in part, by Grant CA114021 (A.G.) from the National Cancer Institute, National Institutes of Health.

Supporting Information Available: Results from elemental analyses. This material is available free of charge via the Internet at http://pubs.acs.org.

References

(1) Presented in part at the 232nd American Chemical Society (ACS) National Meeting in San Francisco, CA, Sept. 10−14, 2006; MEDI number 142.

(2) Jordan, M. A.; Wilson L. Microtubules as a Target for Anticancer Drugs. *Nat. Rev. Cancer* **2004**, *4*, 253−265.

(3) Heald, R.; Nogales, E. Microtubule Dynamics. *J. Cell Sci.* **2002**, *115*, 3−4.

(4) Rowinsky, E.; Donehower, R. C. Antimicrotubule Agents. In *Cancer. Principles and Practice of Oncology*, 6th ed.; DeVita, V. T., Hellman S., Rosenburg, S. A., Eds.; Lippincott-Raven: Philadelphia, PA, 2001; pp 431−452.

(5) Löwe, J.; Li, H.; Downing, K. H.; Nogales, E. Refined Structure of $\alpha\beta$-Tubulin at 3.5 Å Resolution. *J. Mol. Biol.* **2001**, *313*, 1045−1057.

(6) Ravelli, R. B. G.; Gigant, B.; Curmi, P. A.; Jourdain, I.; Lachkar, S.; Sobel, A.; Knossow, M. Insight into Tubulin Regulation from a Complex with Colchicine and a Stathmin-like Domain. *Nature* **2004**, *428*, 198−202.

(7) Tozer, G. M.; Kanthou, C.; Parkins, C. S.; Hill, S. A. The Biology of the Combretastatins as Tumour Vascular Targeting Agents. *Int. J. Exp. Pathol.* **2002**, *83*, 21−38.

(8) Prise, V. E.; Honess, D. J.; Stratford, M. R.; Wilson, J.; Tozer, G. M. The Vascular Response of Tumor and Normal Tissues in the Rat to the Vascular Targeting Agent. Combretastatin A-4-Phosphate at Clinically Relevant Doses. *Int. J. Oncol.* **2003**, *21*, 717−726.

(9) Sikic, B.; Fisher, G.; Lum, B.; Halsey, J.; Beketic-Oreskovic, L.; et al. Modulation and Prevention of Multidrug Resistance by Inhibitors of P-Glycoprotein. *Cancer Chemother. Pharmacol.* **1997**, *40*, S13−S19.

(10) Ling, V. Multidrug Resistance: Molecular Mechanisms and Clinical Relevance. *Cancer Chemother.* **1997**, *40*, S3−S8.

(11) Tan, B. Multidrug Resistance Transporters and Modulation. *Appl. Biochem. Biotechnol.* **2000**, *87*, 233−245.

(12) Grant, C. E.; Valdimarsson, G.; Hipfner, D. R.; Almquist, K. C.; Cole, S. P.; et al. Overexpression of Multidrug Resistance-Associated Protein (MRP) Increases Resistance to Natural Product Drugs. *Cancer Res.* **1994**, *54*, 357−361.

(13) Kruh, G. D.; Chan, A.; Myers, K.; Gaughan, K.; Miki, T.; Aaronson, S. A. Expression Complementary DNA Library Transfer Establishes MRP as a Multidrug Resistance Gene. *Cancer Res.* **1994**, *54*, 1649−1652.

(14) Cole, S. P.; Bhardwaj, G.; Gerlach, J. H.; Mackie, J. E.; Grant, C. E.; et al. Overexpression of a Transporter Gene in a Multidrug-Resistant Human Lung Cancer Cell Line. *Science* **1992**, *258*, 1650−1654.

(15) Horio, M.; Gottesman, M.; Pastan, I. ATP-Dependent Transport of Vinblastine in Vesicles from Human Multidrug-Resistant Cells. *Proc. Natl. Acad. Sci.* **1988**, *85*, 3580−3584.

(16) Goldstein, L. J.; Galski, H.; Fojo, A.; Willingham, M.; Lai, S. L.; et al. Expression of a Multidrug Resistance Gene in Human Cancers. *J. Natl. Cancer Inst.* **1989**, *81*, 116−124.

(17) Fojo, A. T.; Ueda, K.; Slamon, D. J.; Poplack, D. G.; Gottesman, M. M. Pastan, I. Expression of a Multidrug-Resistance Gene in Human Tumors and Tissues. *Proc. Natl. Acad. Sci.* **1987**, *84*, 265−269.

(18) Bell, D. R.; Gerlach, J. H.; Kartner, N.; Buick, R. N.; Ling, V. Detection of P-Glycoprotein in Ovarian Cancer: A Molecular Marker Associated With Multidrug Resistance. *J. Clin. Oncol.* **1985**, *3*, 311−315.

(19) Ma, D. D.; Scurr, R. D.; Davey, R. A.; Mackertich, S. M.; Harman, D. H.; et al. Detection of a Multidrug Resistant Phenotype in Acute Non-Lymphoblastic Leukaemia. *Lancet* **1987**, *1*, 135−137.

(20) van de Vrie, W.; Marquet, R. L.; Stoter, G.; De Bruijn, E. A.; Eggermont, A. M. In Vivo Model Systems in P-Glycoprotein-Mediated Multidrug Resistance. *Crit. Rev. Clin. Lab. Sci.* **1998**, *35*, 1−57.

(21) Trock, B. J.; Leonessa, F.; Clarke, R. Multidrug Resistance in Breast Cancer: A Meta-Analysis of MDR1/gp170 Expression and Its Possible Functional Significance. *J. Natl. Cancer Inst.* **1997**, *89*, 917−931.

(22) Nooter, K.; Westerman, A. M.; Flens, M. J.; Zaman, G. J.; Scheper, R. J.; van Wingerden, K. E.; Burger, H.; Oostrum R.; Boersma, T.; Sonneveld, P. Expression of the Multidrug Resistance-Associated Protein (MRP) Gene in Human Cancers. *Clin. Cancer Res.* **1995**, *1*, 1301−1310.

(23) Schadendorf, D.; Makki, A.; Stahr, C.; van Dyck, A.; Wanner, R.; Scheffer, G. L.; Flens, M. J.; Scheper, R.; Henz, B. M. Membrane Transport Proteins Associated With Drug Resistance Expressed in Human Melanoma. *Am. J. Pathol.* **1995**, *147*, 1545−1552.

(24) Hart, S. M.; Ganeshaguru, K.; Hoffbrand, A. V.; Prentice, H. G.; Mehta, A. B. Expression of the Multidrug Resistance-Associated Protein (MRP) in Acute Leukaemia. *Leukemia* **1994**, *8*, 2163−2168.

(25) Tsuruo, T.; Iida, H.; Tsukagoshi, S.; Sakurai, Y. Overcoming of Vincristine Resistance in P388 Leukaemia In Vivo and In Vitro Through Enhanced Cytotoxicity of Vincristine and Vinblastine by Verapamil. *Cancer Res.* **1981**, *41*, 1967−1972.

(26) Martin, C.; Berridge, G.; Mistry, P.; Higgins, C.; Charlton, P.; Callaghan, R. The Molecular Interaction of the High Affinity Reversal Agent XR9576 with P-Glycoprotein. *Br. J. Pharmacol.* **1999**, *128*, 403−411.

(27) Stewart, A.; Steiner, J.; Mellows, G.; Laguda, B.; Norris, D.; Bevan, P. Phase I Trial of XR9576 in Healthy Volunteers Demonstrates Modulation of P-Glycoprotein in CD56+ Lymphocytes After Oral and Intravenous Administration. *Clin. Cancer Res.* **2000**, *6*, 4186−4191.

(28) Dantzig, A. H.; Shepard, R. L.; Cao, J.; Law, K. L.; Ehlhardt, W. J.; Baughman, T. M.; Bumol, T. F.; Starlinig J. J. Reversal of P-Glycoprotein-Mediated Multidrug Resistance by a Potent Cyclopropyldibenzosuberane Modulator, LY335979. *Cancer Res.* **1996**, *56*, 4171−4179.

(29) Avendaño, C.; Menéndez, J. C. Inhibitors of Multidrug Resistance to Antitumor Agents (MDR). *Curr. Med. Chem.* **2002**, *9*, 159−193.

(30) Pajeva, I. K.; Globisch, C.; Wiese, M. Structure−Function Relationships of Multidrug Resistance P-Glycoprotein. *J. Med. Chem.* **2004**, *47*, 2523−2533.

(31) Gombar, V. K.; Polli, J. W.; Humphreys, J. E.; Wring, S. A.; Serabjit-Singh, C. S. Predicting P-Glycoprotein Substrates by a Quantitative Structure−Activity Relationship Model. *J. Pharm. Sci.* **2004**, *93*, 957−968.

(32) Seigneuret, M.; Garnier-Suillerot, A. A Structural Model for the Open Conformation of the MDR1 P-glycoprotein Based on the MsbA Crystal Structure. *J. Biol. Chem.* **2003**, *32*, 30115−30124.

(33) Rosenbuerg, M. F.; Kamis, A. B.; Callaghan, R.; Higgins, C. F.; Ford, R. C. Three-Dimensional Structures of the Mammalian Multidrug Resistance P-Glycoprotein Demonstrate Major Conformational Changes in the Transmembrane Domains Upon Nucleotide Binding. *J. Biol. Chem.* **2003**, *278*, 8294−8299.

(34) Gangjee, A.; Yang, J.; Ihnat, M. A.; Kamat, S. Antiangiogenic and Antitumor Agents: Design, Synthesis and Evaluation of Novel 2-Amino-4-(3-bromoanilino)-6-benzylsubstituted Pyrrolo[2,3-*d*] Pyrimidines as Inhibitors of Receptor Tyrosine Kinases. *Bioorg. Med. Chem.* **2003**, *11*, 5155−5170.

(35) Gangjee, A.; Zeng, Y.; Ihnat, M.; Warnke, L. A.; Green, D. W.; Kisliuk, R. L.; Lin, F.-T. Novel 5-Substituted 2,4-Diaminofuro[2,3-*d*]pyrimidines as Multi-Receptor Tyrosine Kinase and Dihydrofolate Reductase Inhibitors with Antiangiogenic and Antitumor Activity. *Bioorg. Med. Chem.* **2005**, *13*, 5475−5491.

(36) Gangjee, A.; Zeng, Y.; McGuire, J. J.; Kisliuk, R. L. Synthesis of Classical, Four-Carbon-Bridged 5-Substituted Furo[2,3-*d*]pyrimidine and 6-Substituted Pyrrolo[2,3-*d*]pyrimidine Analogues as Antifolates. *J. Med. Chem.* **2005**, *48*, 5329−5336.

(37) Gangjee, A.; Qiu, Y.; Kisliuk, R. L. Synthesis of Classical and Nonclassical 2-Amino-4-oxo-6-benzythieno[2,3-*d*]pyrimidines as Potential Thymidylate Synthase Inhibitors. *J. Heterocycl. Chem.* **2004**, *41*, 941−946.

(38) Gangjee, A.; Jain, H. D.; Phan, J.; Lin, X.; Song, X.; McGuire, J. J.; Kisliuk, R. L. Dual Inhibitors of Thymidylate Synthase and Dihydrofolate Reductase as Antitumour Agents: Design, Synthesis, and Biological Evaluation of Classical and Nonclassical Pyrrolo[2,3-*d*]-pyrimidine Antifolates. *J. Med. Chem.* **2006**, *49*, 1055−1065.

(39) Garcia-Echeverria, C.; Fabbro, D. Therapeutically Targeted Anticancer Agents: Inhibitors of Receptor Tyrosine Kinases. *Mini-Rev. Med. Chem.* **2004**, *4*, 273−283.

(40) Gangjee, A.; Yu, J.; McGuire, J. J.; Cody, V.; Galitsky, N.; Kisliuk, R. L.; Queener, S. F. Design, Synthesis, and X-ray Crystal Structure of a Potent Dual Inhibitor of Thymidylate Synthase and Dihydrofolate Reductase as an Antitumor Agent. *J. Med. Chem.* **2000**, *43*, 3837−3851.

(41) We thank the National Cancer Institute for performing the in vitro antitumor evaluation in their 60 tumor preclinical screening program.

(42) (a) Boyd, M. R. In *Cancer: Principles and Practice of Oncology*; DeVita, V. T. Jr., Hellman, S., Resenberg, S. A., Eds.; Lippincott: Philadelphia, PA, 1989; Vol. 3, pp 1−12. (b) Boyd, M. R.; Paull, K.

D.; Rubinstein, L. R. In *Cytotoxic Anticancer Drugs: Models and Concepts for Drug Discovery and Development*; Vleriote, F. A., Corbett, T. H., Baker, L. H., Eds.; Kluwer Academic: Hingham, MA, 1992; pp 11−34.

(43) (a) Bai, R.; Paull, K. D.; Hearld, C. L.; Pettit, G. R.; Hamel, E. Halichondrin B and Homohalichondrin B, Marine Natural Products Binding in the *Vinca* Domain of Tubulin. Discovery of Tubulin-Based Mechanism of Action by Analysis of Differential Cytotoxicity Data. *J. Biol. Chem.* **1991**, *266*, 15882−15889. (b) Paull, K. D.; Lin, C. M.; Malspeis, L.; Hamel, E. Identification of Novel Antimitotic Agents Acting at the Tubulin Level by Computer-Assisted Evaluation of Differential Cytotoxicity Data. *Cancer Res.* **1992**, *52*, 3892−3900.

(44) Paull, K. D.; Hamel, E.; Malspeis, L. The Prediction of Biochemical Mechanism of Action From the In Vivo Antitumor Screen of the National Cancer Institute. In *Cancer Chemotherapeutic Agents*; Foye, W. O., Eds.; American Chemical Society: Washington DC, 1995; pp 9−45.

(45) Smith, C. D.; Zhang, X. Mechanism of Action of Cryptophycin. Interaction With the Vinca Alkaloid Domain of Tubulin. *J. Biol. Chem.* **1996**, *271*, 6192−6198.

(46) Schneider, E.; Horton, J. K.; Yang, C. H.; Nakagawa, M.; Cowan, K. H. Multidrug Resistance-Associated Protein Gene Overexpression and Reduced Drug Sensitivity of Topoisomerase II in a Human Breast Carcinoma MCF7 Cell Line Selected for Etoposide Resistance. *Cancer Res.* **1994**, *54*, 152−158.

(47) Smith, C. D.; Zilfou, J. T.; Stratmann, K.; Patterson, G. M. L.; Moore, R. E. Welwitindolinone Analogues That Reverse P-glycoprotein-Mediated Multiple Drug Resistance. *Mol. Pharm.* **1995**, *47*, 241−247.

(48) Smith, C. D.; Zilfou, J. T. Circumvention of P-Glycoprotein-Mediated Multiple Drug Resistance by Phosphorylation Modulators is Independent of Protein Kinases. *J. Biol. Chem.* **1995**, *270*, 28145−28152.

(49) Zilfou, J. T.; Smith, C. D. Differential Interactions of Cytochalasins with P-Glycoprotein. *Oncol. Res.* **1995**, *7*, 435−443.

(50) Zhang, X.; Smith, C. D. Microtubule Effects of Welwistatin, A Novel Cyanobacterial Indolinone That Circumvents Multiple Drug Resistance. *Mol. Pharm.* **1996**, *49*, 288−294.

(51) Lawrence, D. L.; Copper, J. E.; Smith, C. D. Structure−Activity Studies of Substituted Quinoxalinones as Multiple Drug Resistance Antagonists. *J. Med. Chem.* **2001**, *44*, 594−601.

(52) Smith, C. D.; Myers, C. B.; Zilfou, J. F. Smith, S. N.; Lawrence, D. S. Indoloquinoxaline Compounds that Selectively Antagonize P-Glycoprotein. *Oncol. Res.* **2001**.

(53) Lee, B. D.; Li, Z. -J.; French, D. J.; Zhuang, Y.; Xia, Z.; Smith, C. D. Synthesis and Evaluation of Novel Dihydropyrroloquinolines that Selectively Antagonize P-Glycoprotein. *J. Med. Chem.* **2004**, *47*, 1413−1422.

(54) Skehan, P.; Stoneng, R.; Scudiero, D.; Monks, A.; McMahon, J.; Vistica, D.; Warren, J. T.; Bokesch, H.; Kenney, S.; Boyd, M. R. New Colorimetric Cytotoxicity Assay for Anticancer-Drug Screening. *J. Natl. Cancer Inst.* **1990**, *82*, 1107−1112.

(55) Vindelov, L. L.; Christensen, I. J.; Nissen, N. I. A Detergent-Trypsin Method for the Preparation of Nuclei for Flow Cytometric DNA Analysis. *Cytometry* **1983**, *3*, 323−327.

(56) Vallee, R. B. Reversible Assembly Purification of Microtubules Without Assembly-Promoting Agents and Further Purification of Tubulin, Microtubule-Associated Proteins, and MAP Fragments. *Methods Enzymol.* **1986**, *134*, 89−104.

(57) Bai, R.; Pettit, G. R.; Hamel, E. Dolastatin 10, a Powerful Cytostatic Peptide Derived from a Marine Animal. Inhibition of Tubulin Polymerization Mediated Through the Vinca Alkaloid Binding Domain. *Biochem. Pharmacol.* **1990**, *39*, 1941−1949.

JM070194U